Supplementary Information

Could the Rising Star hominins represent relict australopiths?

Clément Zanolli[1,2,*]

[1] *Univ. Bordeaux, CNRS, MCC, PACEA, UMR 5199, F-33600 Pessac, France*

[2] *Evolutionary Studies Institute, University of the Witwatersrand, 1 Jan Smuts Avenue, Johannesburg, South Africa*

*e-mail: clement.zanolli@gmail.com

Supplementary Note 1

Taxonomic value of the craniodental metric and non-metric features used by Berger et al. (Ref. 1: Supplementary file 2) and Hawks et al. (Ref. 2)

The taxonomic significance of the craniodental traits described as diagnostic of Homo by Berger et al.[1] and Hawks et al.[2]. A number of features were regarded as diagnostic of *Homo* (i.e., autapomorphies) in these previous studies, but their presence in various specimens attributed to *Australopithecus* and/or *Paranthropus* (i.e., representing either symplesiomorphies or homoplasies) make them taxonomically irrelevant at genus level (Supplementary Table S1). Based on the list of features provided by Berger et al. (Ref. 1: Supplementary file 2) and on the selected features illustrated in Hawks et al. (Ref 2: Figure 34), the Rising Star hominins seem to have more in common with *Homo* than with the australopiths. Several cranial traits were previously reported to be typical of our own genus: absence of sagittal crest, overall gracile morphology, reduced postorbital constriction, morphology of the frontal, parietal and occipital bones, origin of the zygomatic bone on the temporal bone, arched supraorbital torus, and absence of anterior pillar[1,2]. However, many of these trait are in fact not diagnostic as they can be found in specimens belonging to two or three hominin genera (*Australopithecus*, *Paranthropus* and *Homo*). In addition, due to the incompleteness of the face (in particular of the orbits and zygomatic bone), and to the lack of anatomical connection between the neurocranium and face of the Rising Star crania, some features like the supraorbital height index, should be interpreted with caution.

Several metric and non-metric traits were compared in various hominin taxa and include the endocranial volume, the postorbital constriction index, the postorbital breadth/biparietal breadth index, the origin of the zygomatic process, the index of palate protrusion, the index of maxilloalveolar length/breadth, the corpus shape index, the P_3 root morphology, the orientation of the M_3 distal root (individual data are reported in Supplementary Tables S1–S10). The postorbital breadth/biparietal breadth index was computed as follows: postorbital breadth index/biparietal breadth × 100. The index of palate protrusion evaluates the proportion of the palate that is anterior to sellion and is a measure of facial prognathism. It is computed as follows: horizontal distance between nasospinale and vertical projection perpendicular to the sellion/horizontal distance between nasospinale and M_3 × 100. The index of maxilloalveolar length/breadth was computed as follows: maxilloalveolar length/ maxilloalveolar breadth × 100. The mandible

corpus shape index was calculated based on measurements of breadth and height of the corpus at M_1 position. This index used to compare variation in hominoid corpus 'robusticity' was computed as follows: breadth/height × 100. The adjusted Z-scores comparing corpus shape index were computed for each of the Rising Star specimens in comparison with mandibles of *Australopithecus*, *Paranthropus* and *Homo* species/samples based on the sample size, mean, and standard deviation of the latter taxon following Scolan and collaborators[50]. This method allows the comparison of small and unbalanced samples by using the Student's t inverse distribution, where the –1.0 to +1.0 interval comprises 95% of the variation in the reference sample.

The anteroposterior variations of cranial breath were quantified by using the postorbital constriction index and the postorbital breadth/biparietal breadth ratio. These two indices show substantial overlap between the Rising Star hominins, *Australopithecus*, *Paranthropus* and Pleistocene *Homo*, and even if postorbital constriction is less marked than in most australopith taxa, it is within the range of *P. robustus* (Supplementary Table S1).

Cranial capacity of the Rising Star hominins is inferior to most species of *Homo* (expect *H. floresiensis* and some *H. habilis* specimens) and on par with the australopith condition (Supplementary Table S1). Cranial vault thickness of the Rising Star hominins is described as thin, and overlaps with all reported hominid taxa (Ref. 1: Supplementary file 2). In fact, cranial vault thickness is highly variable depending on the area where it is measured and it was also shown to be variable at intra- and inter-taxic level[51]. The absence of a sagittal crest and the gracile facial morphology of the Rising Star hominins, in particular in the holotype DH1, were described to be distinct from species of the genus *Paranthropus*[1], but some *Paranthropus robustus* specimens, like DNH 7 from Drimolen, have no sagittal crest and show less robust traits[40,41]. The endocasts of DH1 and DH3 were described as showing a *Homo*-like configuration of the fronto-orbital region, but no detailed comparisons with *Paranthropus* were conducted by Holloway and collaborators[52]. A more recent study by Hurst et al.[53] described an absolutely and large third frontal convolution area, which would indicate the presence of an enlarged Broca area in the Rising Star hominins and possibly have implications for vocal communication. However, this anatomical trait is found in all hominids and its area largely depends on brain size, meaning that it has little to no taxonomic value. Considering the large variation in the expansion of this feature in Early to Middle Pleistocene *Homo*, even the functional aspects should be interpreted with caution[54].

Supraorbital height index is reported by Berger et al. (Ref. 1: Supplementary file 2) to be high, but considering the lack of face in the most complete crania DH1 and DH3, it is unclear how this index was measured or assessed.

In some cases, traits like the presence of a supraorbital torus and supratoral sulcus were described as typical of *Homo*, even if they are substantially less developed than in *H. erectus* and any other Middle Pleistocene species of *Homo*[1,2,8]. In fact, these facial features are not clearly expressed in the Rising Star fossils, and the supraorbital morphology of DH1 is not much different from that seen in some australopiths like Sts 5.

A reduced postorbital constriction can be found in both *Australopithecus* and early *Homo* (including specimens generally attributed to *H. habilis*, *H. rudolfensis* and *H. erectus* s.l.), as attested by the postorbital constriction index (ranging between 0.72 and 0.81 in these taxa; Supplementary Tables S1 and S3). The proportions of the neurocranium in the Rising Star hominins are difficult to assess (especially the maximal breadth and height) because no complete cranium has been recovered yet and reconstructions are potentially prone to error (which could, to a lesser extent, also affect reconstructions of endocranial volume; Supplementary Table S1; see also Ref. 2). However, accepting such estimates as potentially informative, the few indices based on linear measurements that can be computed on the Rising Star crania are not taxonomically diagnostic. As attested by the ratio of postorbital breadth by biparietal breadth, the three genera overlap and range between 59.1 and 71.0, encompassing the value of 66.0 of the Rising Star reconstructed crania (Supplementary Tables S1 and S4). The postorbital constriction index value for the Rising Star hominins (79.1) is also within the range of *Australopithecus* and early *Homo*, and is just above that of *Paranthropus* (Supplementary Table S1). The size and shape of the supraorbital torus are also highly variable among *Australopithecus*, *Paranthropus* and *Homo*, in relation to several factors including sexual dimorphism, ontogeny and intra-taxic variation due to chronogeographic distribution[1,55].

Frontal bossing is a subjective trait to score. As shown by the geometric morphometric analyses of the cranial vault, the shape of the frontal and of the neurocranium of the Rising Star hominins is more similar to that of *Paranthropus* than to *Homo* (Fig. 1a). Similarly, parietal bossing is not evident on the published photos (Ref. 2: Fig. 2) or on the 3D surface models available on MorphoSource (http://www.morphosource.org), and the neurocranium profile in posterior view resembles more the australopith condition (Fig. 1b).

Metopic keeling is reported as absent in all of the taxa investigated by Berger et al. (Ref. 1: Supplementary file 2) and is thus uninformative. Sagittal keeling is recorded in the Rising Star hominins, but also in *Paranthropus* and in some *Homo erectus* specimens (Ref. 1: Supplementary file 2). The parietal walls of the Rising Star hominins are described as vertical but as shown in Berger et al. (Ref. 1: Fig. 2), the holotype DH1 shows superiorly tapering parietal walls, like in the australopiths (see also Fig. 1b). According to Berger et al. (Ref. 1: Supplementary file 2), the postbregmatic depression is found in most hominin taxa, and is thus non-diagnostic, prelambdoidal flattening is present in both *Paranthropus* and *Homo*, but not in *Australopithecus* and the temporal crest is reported to be in posterior position with respect to the supraorbital torus, as in some species of *Australopithecus* and *Homo*, meaning again that it is not a typical feature of *Homo*.

Anteromedial incursion of temporal lines is weak as in most species of *Homo*, but as also seen in *Australopithecus* sediba, while *Paranthropus* and other species of *Australopithecus* have more medially located temporal lines in general (Ref. 1: Supplementary file 2). The position of this line is related to the development of the temporalis muscle that attaches to this structure and to functional adaptations related to dietary behavior, meaning that not a taxonomic diagnostic trait (for example, the position of the temporal line varies from weak to strong in *Pan troglodytes*; Ref. 1: Supplementary file 2). Compound temporal/nuchal crest is absent as in all species of *Homo*, but also as in *Paranthropus robustus*, *Australopithecus africanus* and *A. sediba* (Ref. 1: Supplementary file 2). Temporal squama height is described to be low, the upper margin of the temporal squama is described as curved and the supramastoid crest is reported to be marked as in most hominin taxa (Ref. 1: Supplementary file 2).

An angular torus is described in the Rising Star hominins as in Early Pleistocene *Homo*, and reported to be absent in *Australopithecus* and *Paranthropus* (Ref. 1: Supplementary file 2), but this is incorrect as it was previously described in australopith specimens such as Sts 5 and OH 5 for example[56].

The point of lateral expansion of the root of the zygomatic is described to be above the mandibular fossa in the Rising Star hominins (Ref. 1: Supplementary file 2), as in all species of *Homo* and *A. sediba*, but the same condition is also found in the *Paranthropus* specimen DNH 7[41]. In addition, the morphology of the zygomatic root on the temporal bone of LES1 shows that it originates above the external auditory meatus[2], as in the australopiths (Ref. 1: Supplementary

file 2). Similarly the angulation of the root of the zygomatic is described to be angled, as in Early Pleistocene *Homo* (Ref. 1: Supplementary file 2), but the LES1 specimen shows a parallel condition[2], as in the australopiths and some early *Homo* specimens.

The projection of the mastoid crest, the orientation of the mastoid and supramastoid crests and the plate-like tympanic shape are not diagnostic as the same condition is found in *Homo* and the australopiths (Ref. 1: Supplementary file 2). A small suprameatal spine is present in the Rising Star hominins, as in most Pleistocene *Homo* specimens and in some *Paranthropus* and *Australopithecus* crania (Ref. 1: Supplementary file 2). The mandibular fossa in moderately deep and the articular tubercle is not or slightly projecting, as it can be observed in representatives of the three hominin genera (Ref. 1: Supplementary file 2). The postglenoid process is small, as in *Homo* and *Paranthropus* (Ref. 1: Supplementary file 2). The postglenoid and tympanic contact and the entoglenoid process is projecting, as found in most hominin species (Ref. 1: Supplementary file 2).

The position of the mandibular fossa relative to temporal squama is described to be medial, as in all species of *Homo*, *A. sediba* (Ref. 1: Supplementary file 2), but also as in the *A. africanus* specimen Sts 5 (pers. observation). The vaginal process of the temporal bone is absent or small in the Rising Star hominins and described as moderate to large in *Paranthropus* (Ref. 1: Supplementary file 2), but some specimens like DNH 7 shows a small and thin vaginal process[41]. The Eustachian process of the tympanic is described as present and prominent in the Rising Star hominins, as in *Australopithecus* and *Paranthropus*, while it is absent or slightly developed in *Homo* (Ref. 1: Supplementary file 2). The petrous bone is coronally oriented, as in *Homo* and *Paranthropus*, while *Australopithecus* tends to show a more intermediate orientation (Ref. 1: Supplementary file 2). The external auditory meatus is supposedly small in the Rising Star hominins, but this is subjective and it does not appear to be proportionally smaller than in some *Paranthropus* specimens like DNH 7[41]. The position and orientation of the external auditory meatus is not a diagnostic trait as the same condition is found in all three hominin genera (Ref. 1: Supplementary file 2).

The crista petrosa is absent or weakly expressed in the Rising Star hominins and in some *Australopithecus* specimens, and moderate to strong in *Homo*, and supposedly also in *Paranthropus* (Ref. 1: Supplementary file 2), but it is weakly developed in the *Paranthropus* specimen DNH 7[41]. The mastoid process of the Rising Star hominins is inflated, as in most

australopiths, while it is not in *Homo* (except in some *H. habilis* fossils; Ref. 1: Supplementary file 2). The fossa at the origin of the digastric muscle is deep and forms a narrow notch, as in *P. robustus*, *H. habilis* and *H. sapiens* (Ref. 1: Supplementary file 2). The juxtamastoid eminence and occipito-mastoid crest are present, while the asterionic notch is absent, as in a number of hominin species of the three genera (Ref. 1: Supplementary file 2). The occipital torus is present as in *Australopithecus*, *Paranthropus* and most species of *Homo* (Ref. 1: Supplementary file 2).

The curvature of the occipital squama and of the nuchal plane are described to be resembling the condition of *Homo* and to differ from *Australopithecus* and *Homo*, but the geometric morphometric analyses conducted in this work that capture the morphology of the lateral occipital profile show that the Rising Star hominins differ from *Homo* and better approximate the morphology of *Paranthropus* (Fig. 1a). The nuchal plane is low and near to or below the Frankfort horizontal plane in the Rising Star hominins, as in most hominin species (Ref. 1: Supplementary file 2). The external occipital protuberance is present as in *H. habilis* and *P. robustus*, while it is absent in most of the other hominin species (Ref. 1: Supplementary file 2). The tuberculum linearum and the external occipital crest are present, and the occipital torus and supramastoid crest do not contact in a continuous way, as in species of the three hominin genera (Ref. 1: Supplementary file 2).

Supraorbital torus/arch thickness is intermediate, as in various species of the three genera (Ref. 1: Supplementary file 2). The supraorbital thickness gradient is medial to lateral in the Rising Star hominins as in some *Australopithecus* species, and for most species of *Homo*, while the opposite is reported for *Paranthropus* (Ref. 1: Supplementary file 2), but DNH 7 shows the same condition as the Rising Star hominins[41]. A supratoral sulcus is present in the Rising Star hominins, as in *A. sediba*, *H. habilis*, *H. erectus*, while it is absent in *Paranthropus*, and a supraorbital torus is present as in several species of the three genera (Ref. 1: Supplementary file 2). The supraorbital contour is described as weakly arched, but it is a subjective assessment and does not differ from the morphology of the australopiths or of early *Homo*. Same for the supraorbital corner shape, described as rounded, as in most hominin taxa (Ref. 1: Supplementary file 2). The presence of a canine fossa in the Rising Star hominins is also variably observed in most hominin taxa (Ref. 1: Supplementary file 2). There is no anterior pillar in the Rising Star hominins, as in most species of *Homo*, *A. sediba*, *P. aethiopicus*, *P. boisei* and a number of *P. robustus* specimens (e.g., DNH 7, SK 52/SKW 18, SKW 11)[1,41]. The incisors project beyond the

bicanine line, as in *Australopithecus*, *Paranthropus* and *Homo* (Ref. 1: Supplementary file 2 states that it is not the case in *Paranthropus*, which is incorrect[41]).

The nasoalveolar clivus of LES1 is concave as in the australopiths and in some *H. habilis* specimens, while in Early to Middle Pleistocene *Homo* it tends to be flat to convex/arched (Ref. 1: Supplementary file 2; Supplementary Table S1).

The canine jugum is very weak in the Rising Star hominins, as in *Paranthropus* and *Homo*, while it is more marked in *Australopithecus* (Ref. 1: Supplementary file 2).

The origin of the zygomatic process is at P^3–P^4 level in the Rising Star hominins, a position nearly systematically found in *Paranthropus*, while it is more posteriorly located (generally between P^4 and M^2) in *Australopithecus* and *Homo* (Supplementary Tables S1 and S5).

The intermaxillary suture is described as ridged in the Rising Star hominins, as it is usually the case in *Homo* and in *A. sediba* (Ref. 1: Supplementary file 2), but LES1 shows a furrowed morphology[2], as in *Paranthropus*.

Lateral flaring of the zygomatic arches is slight, as in *A. sediba* and in *Homo*, while *Paranthropus* is describes as having a marked lateral flaring (Ref. 1: Supplementary file 2), but the specimen DNH 7[41] shows a comparable condition to LES1[2]. The zygomatic temporal surface relief is not diagnostic as it is shallow in nearly all hominin taxa (Ref. 1: Supplementary file 2).

The anterior palate is shallow, as in various species of the three hominin genera.
The morphology of the maxilla and mandible of the Dinaledi and Lesedi hominins is anteroposteriorly elongated but also relatively wide mediolaterally as indicated by the maxilloalveolar length/breadth index that overlaps with *Homo* and *Paranthropus* (Ref. 1: Supplementary file 2). The high value for the index of palate protrusion indicates a degree of prognathism exceeding that of Early to Middle Pleistocene *Homo*, but compatible with the australopith condition (Supplementary Tables S1 and S6). Tooth row shape, as reflected in the maxilloalveolar length/breadth index, is proportionally shorter and wider in the Rising Star hominins than in species of *Australopithecus*, but it is within the range of both *Paranthropus* (although at the extreme inferior limit) and Pleistocene *Homo* (Supplementary Tables S1 and S7). The mandible has been described as more gracile than that of *Paranthropus*[1], but the overall morphology (including the corpus height and length, and origin of the ascending ramus) is quite similar. More importantly, corpus proportions of all of the Rising Star mandibles do not statistically differ from those of *P. robustus and A. africanus*, whereas the specimens U.W. 101-

001 and U.W. 101-377 are outside the range of *H. habilis*, *H. erectus* s.l. and/or Middle–Late Pleistocene *Homo* (Supplementary Table S17).

The incisive foramen is located at P^3 level, as in *Australopithecus*, *Paranthropus* and Early to Middle Pleistocene *Homo* (Ref. 1: Supplementary file 2).

The mandibular symphysis area and the cross-sectional area at M_1 are reported to be small (Ref. 1: Supplementary file 2), but this is in absolute terms, and since the Rising Star hominins have small jaws compared with most hominin species, a relative index would be needed to reliably assess the value of this parameter. The inferior transverse torus is more developed than the superior torus, as in *Australopithecus*, *Paranthropus* and several species of *Homo* (Ref. 1: Supplementary file 2). A weak prominent post-incisive planum is shared with several hominin species of the three genera (Ref. 1: Supplementary file 2). The mandibular symphysis is anteriorly vertical, as in *Homo* and *Paranthropus*, whereas is it receding in *Australopithecus* (Ref. 1: Supplementary file 2).

The mental foramen is described as opening posteriorly in the Rising Star hominins (Ref. 1: Supplementary file 2), but is does in fact open laterally in DH1, LES1 and U.W. 101-377[2,3], as in *Australopithecus*, *Paranthropus* and early *Homo* (Ref. 1: Supplementary file 2). It is located at P_3/P_4 level, as it is most frequently the case in hominins and above midcorpus height, as in *P. boisei*, whereas it is generally at midcorpus or below in most hominin taxa (Ref. 1: Supplementary file 2).

The mandibular extramolar sulcus is wide and subalveolar fossae are moderately to prominently expressed, as in most hominin taxa (Ref. 1: Supplementary file 2)

Mandibular incisure is present, as in *A. sediba*, most species of *Homo* (Ref. 1: Supplementary file 2) and some *Paranthropus* specimens (e.g., SK 23).

The Rising Star hominins have molarised premolars, especially the P_3, a condition common in australopiths and in some *H. habilis* and *H. floresiensis* specimens, but not seen in *H. erectus* s.l. and in Middle Pleistocene *Homo* (Supplementary Table S1). The premolars of the Rising Star fossils are multirooted and the P_3 root configuration (2R: MB + D) is found in around 30% of the australopith specimens, but only in two Early Pleistocene *Homo* mandibles (KNM-ER 730 and D2600) and in two *H. floresiensis* specimens (LB1 and LB6; Supplementary Tables S1 and S9)[30,87].

The molars of the Rising Star hominins exhibit inflated bunodont cusps and lower molars with a mesiobuccally restricted protostylid[1,3], traits that are frequent in the australopiths, but rare in *Homo* (a similarly-located protostylid is sometimes present in Chinese *H. erectus*, but differently expressed, forming vertical digitations[57,58]). The distal root of the M_3 of the Rising Star hominins is buccally deflected, a feature only recorded in *P. robustus* and in the specimen SK 15[29], the latter having been recently attributed to *Paranthropus capensis*, a relatively gracile species of *Paranthropus*[42].

The EDJ of post-canines teeth is recognized as a reliable taxonomic proxy[15,,42,59–63], and holds a strong phylogenetic signal[64]. Analyses of the EDJ of the P_3 of the Rising Star hominins show that, while distinct from that of other hominins, it resembles most that of *P. robustus*[28]. The EDJ shape of the Rising Star P_4s is more distinct and intermediate between that of the australopiths and Late Pleistocene *Homo*, but substantially differs from that of *H. erectus*[28]. Future analyses of the EDJ of more teeth of the Rising Star hominins should be able to check the presence of an australopith signature, possibly resembling that of *Paranthropus*.

As summarized in Supplementary Table S1, many craniodental features considered to be diagnostic of *Homo* in the previous studies describing the Rising Star hominins[1,2] actually overlap with other hominin genera. In fact, most of the cranial traits of the Rising Star hominins are either not diagnostic of *Homo*, and for the features that distinguish *Homo* from the other hominins, they are more similar to the australopith condition than to any species of *Homo*.

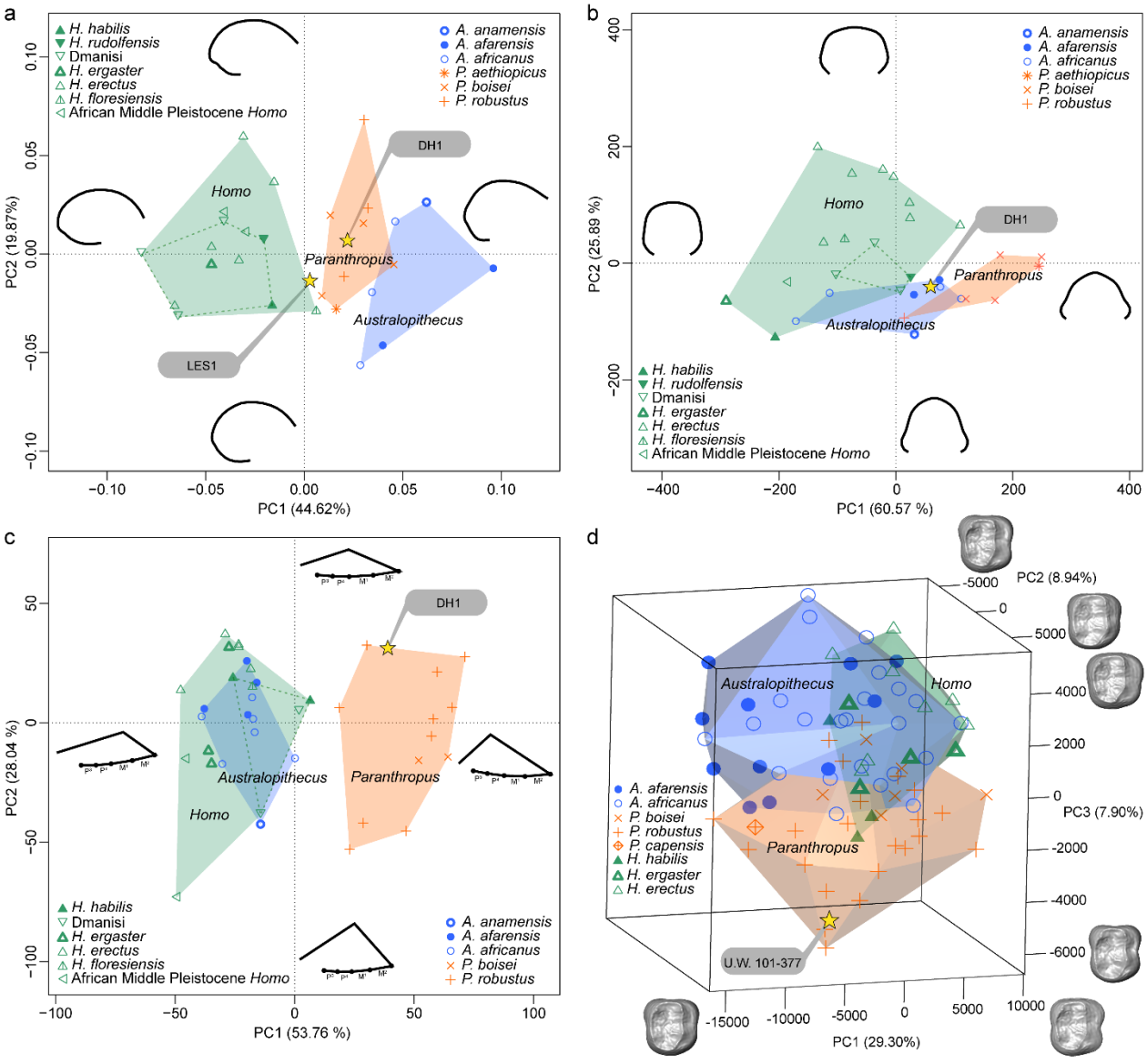

Supplementary Fig. 1. Geometric morphometric analyses of craniodental structures. a–c, Principal component analyses (PCA) of the neurocranium shape in lateral (**a**) and posterior (**b**) views and of the maxilla shape in lateral view (**c**). **d,** PCA of the M_2 enamel-dentine junction. In all analyses, the Rising Star specimens were compared with material representing *Australopithecus*, *Paranthropus* and *Homo* (the list of specimens is reported in Supplementary Tables S11–S13). The dotted convex hulls group taxa/specimens for which their inclusion into *Homo* is debated.

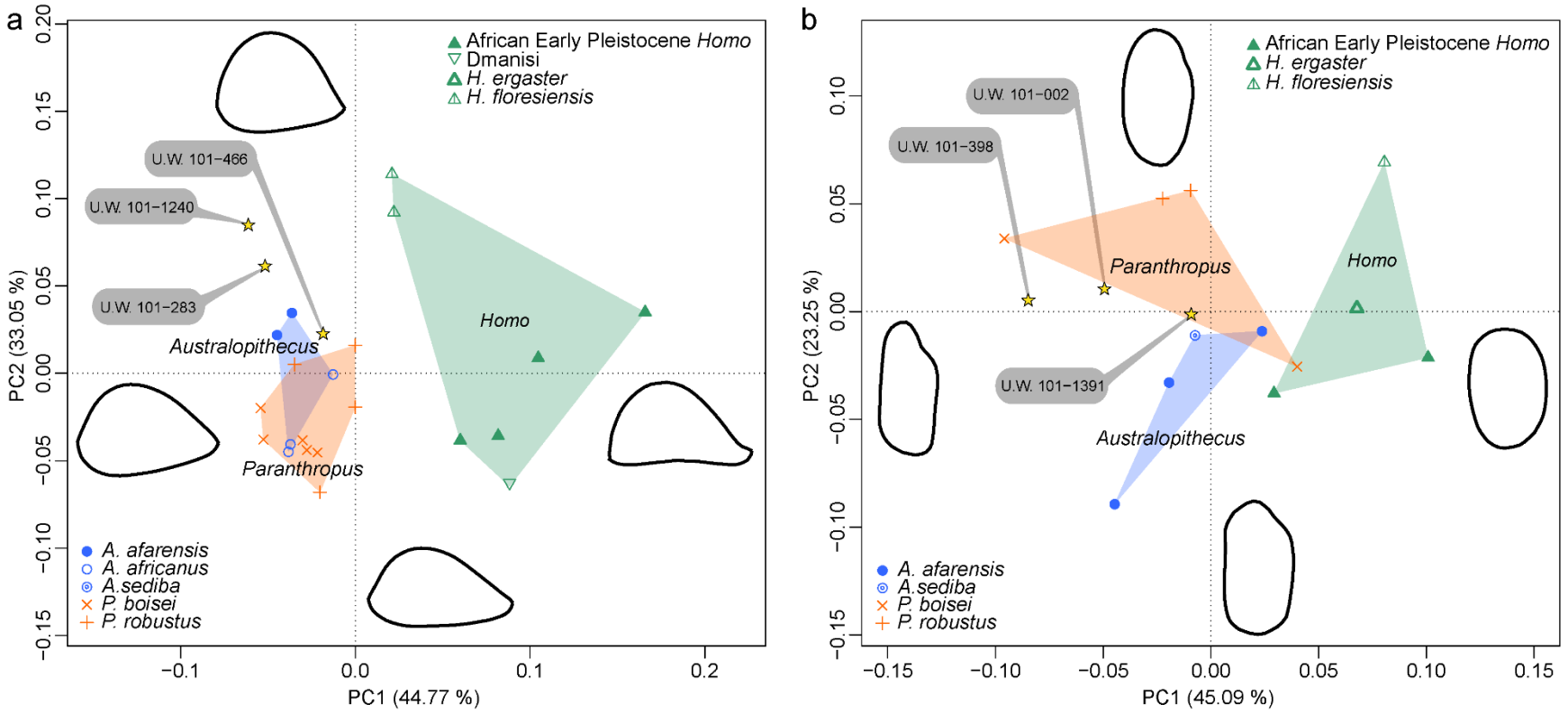

Supplementary Fig. 2. Geometric morphometric analyses of humerus and femur cross-sectional shape. a, b, Principal component analyses of the distal humerus (**a**) and femoral neck (**b**) cross-sections. In all analyses, the Rising Star specimens were compared with material representing *Australopithecus*, *Paranthropus* and *Homo* (the list of specimens is reported in Supplementary Tables S15 and S16).

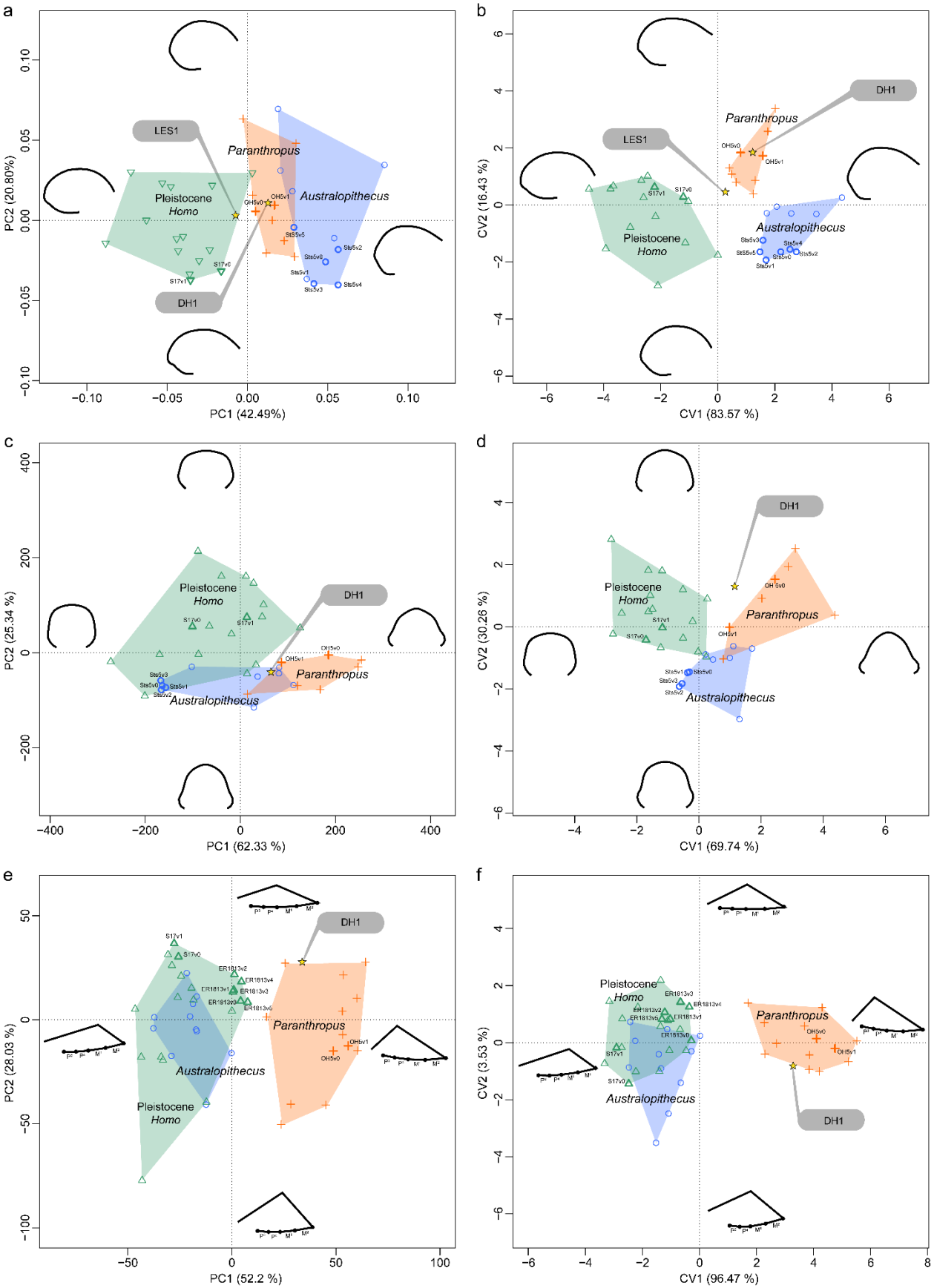
a
PC2 (20.80%)
PC1 (42.49%)
LES1
DH1
Paranthropus
Australopithecus
Pleistocene
Homo
b
CV2 (16.43 %)
CV1 (83.57 %)
c
PC2 (25.34 %)
PC1 (62.33 %)
d
CV2 (30.26 %)
CV1 (69.74 %)
e
PC2 (28.03 %)
PC1 (52.2 %)
f
CV2 (3.53 %)
CV1 (96.47 %)

Supplementary Fig. 3. Influence of tilting and parallax on the geometric morphometric analyses of cranial shape. a, b, Principal component analysis (PCA, **a**) and canonical variate analysis (CVA, **b**) of the neurocranium in lateral view. **c, d,** PCA (**c**) and CVA (**d**) of the neurocranium in posterior view. **e, f,** PCA (**e**) and CVA (**f**) of the maxilla shape in lateral view. In all analyses, the Rising Star specimens DH1 and LES1 were compared with material representing *Australopithecus*, *Paranthropus* and Pleistocene *Homo* (the list of specimens is reported in Supplementary Tables S11 and S12). For the test specimens Sangiran 17 (S17), OH 5 (OH5), Sts 5 (Sts5) and/or KNM-ER 1813 (ER1813), landmarks were placed on published pictures (v0), on screenshots of 3D models aligned along the Frankfurt plane (v1), inferiorly (v2), superiorly (v3), anteriorly (v4), and posteriorly (v5) tilted.

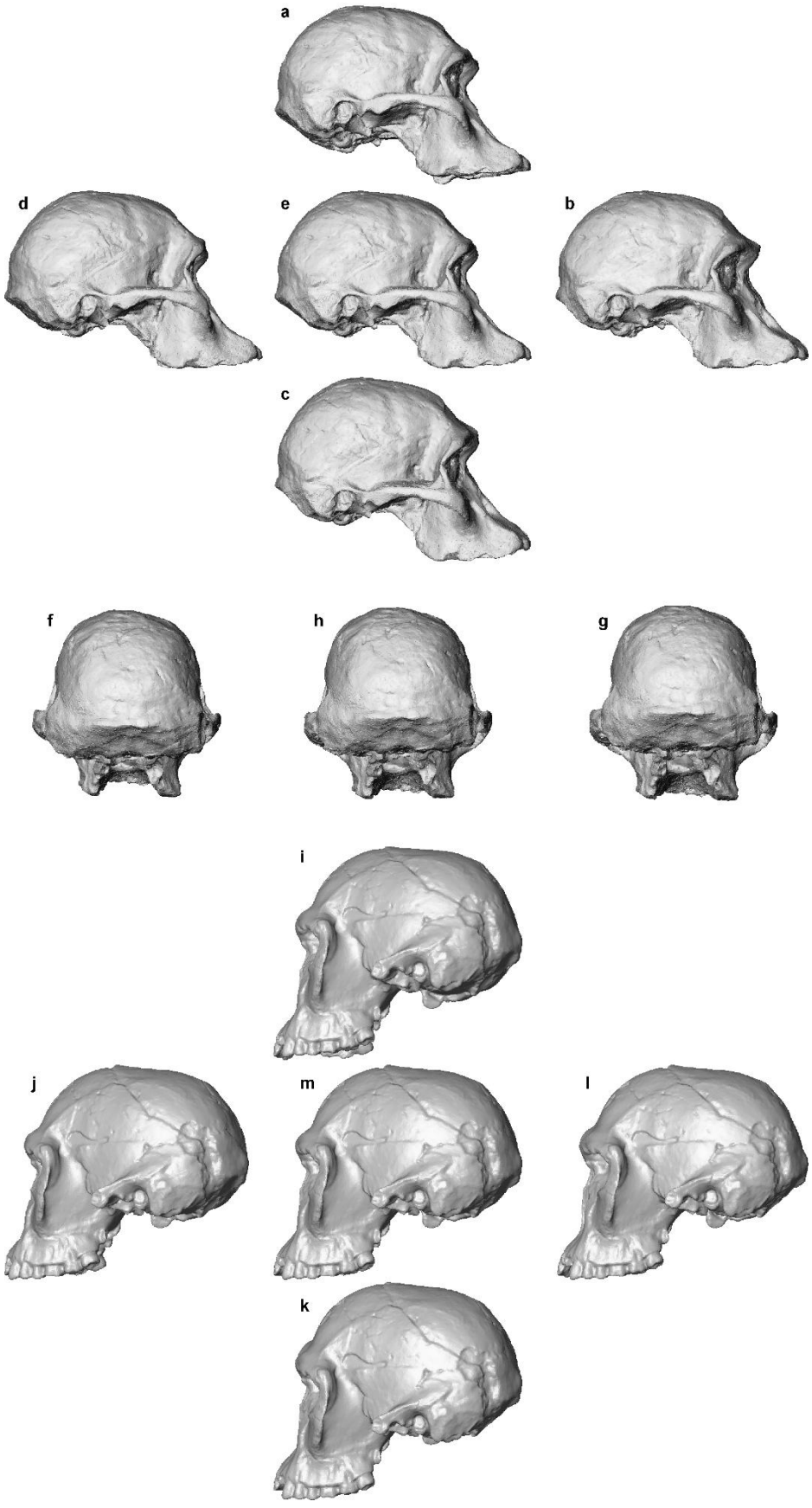
a
d
e
b
c
f
h
g
i
j
m
l
k

Supplementary Fig. 4. Screenshots of 3D models of hominin crania. a–e, Cranium of the specimen Sts 5 in lateral view tilted superiorly (**a**), anteriorly (**b**), inferiorly (**c**), posteriorly (**d**) and aligned along the Frankfurt plane (**e**). **f–h,** Cranium of Sts 5 in posterior view tilted posterosuperiorly (f), anteroinferiorly (g), and aligned along the Frankfurt plane (h). **i–m,** Cranium of the specimen KNM-ER 1813 in lateral view tilted superiorly (**i**), anteriorly (**j**), inferiorly (**k**), posteriorly (**l**) and aligned along the Frankfurt plane (**m**).

Supplementary Table S1. Metric and non-metric craniodental features compared in various hominin taxa.[a]

Trait	Rising Star	*A. afarensis*/ *A. anamensis*	*A. africanus*	*A. sediba*	*P. aethiopicus*	*P. boisei*	*P. robustus*	*H. habilis*	*H. rudolfensis*	*H. erectus* s.l.	Middle Pleistocene *Homo*	*H. floresiensis*
Endocranial volume (cm^3)	465–610	365–550	408–515	420	410–491	390–529	600–750	510–824	752	641–1300	1125–1390	417
Postorbital constriction index (%)	79.1	62.8–64.7	60.9–68.1	81.4	59.0	53.9–67.8	66.4–84.2	69.0	73.6	73.3–89.7	78.4–87.3	69.3
Postorbital breadth/biparietal breadth ×100 (%)	66.0	63.1–74.5	67.4–68.5	73.0	62.0	59.1–67.8	71.0	70.4	65.0	61.0–73.1	67.1–90.4	64.5
Maxilloalveolar length/breadth×100	93	102–111	100–107	100	—	95–105	93–111	91–94	—	90–102	85–94	84.2
Origin of the zygomatic process	P^3–P^4	M^1	M^1	P^4–M^1	P^4–M^1	P^4	P^3–P^4	P^4–M^1	P^4	M^1–M^2	M^1–M^2	M^1
Index of palate protrusion (%)	50	55–59	43–68	43	82	35–53	46	40–48	—	26–48	30–36	37
Corpus shape index (%)	51.7–80.0	48.4–68.9	55.6–83.1	54.8–64.3	—	57.5–76.5	55.6–74.4	58.8–63.0	—	40.5–69.2	58.2–71.0	62.2–73.2
Nasoalveolar clivus	concave	concave	concave	concave	concave	concave	concave	concave–flat	flat	flat–convex	flat–convex	flat
P_3 crown morphology[b]	molarised	singled-cusped–molarised	singled-cusped–molarised	—	molarised?	molarised	molarised	molarised–bicuspid and trigonid≈talonid	—	bicuspid and trigonid≈talonid	bicuspid and trigonid≈talonid	molarised or bicuspid with trigonid≈talonid
P_3 root configuration = 2R: MB + D	7/7	1/1	5/15	—	—	5/11	6/19	0/7	0/1	2/11	0/37	2/3
P_4 crown morphology[b]	molarised	molarised	molarised	—	molarised	molarised	molarised	molarised	—	bicuspid and trigonid≈talonid	bicuspid and trigonid≈talonid	bicuspid and trigonid≈talonid
Buccally-deflected M_3 distal root	5/5	1/1	2/6	—	—	1/2	10/11	0/2	—	0/5	0/2	—

[a] Except for premolar crown morphology, individual data are provided in Supplementary Tables S2–S10.

[b] For these traits, data were extracted from Refs. 1–3.

Supplementary Table S2. List of the fossil material included in the comparison of endocranial volume (ECV).

Specimen	Species/group	ECV (cm^3)	Reference
MRD-VP-1/1	*A. anamensis*	365–370	65
AL 444-2	*A. afarensis*	550	25
Sts 71	*A. africanus*	410	66
Sts 5	*A. africanus*	485	66
StW 505	*A. africanus*	515	67
Sts 60	*A. africanus*	428	67
StW 573	*A. africanus*	408	68
MH 1	*A. sediba*	420	25
KNM-WT 17000	*P. aethiopicus*	410	67
KNM-ER 23000	*P. aethiopicus*	491	25
KNM-WT 17400	*P. boisei*	390	67
KNM-ER 406	*P. boisei*	500	25
KNM-ER 407	*P. boisei*	438–510	25
KNM-ER 732	*P. boisei*	466–500	25
OH 5	*P. boisei*	500–529	25
SK 48	*P. robustus*	750	25
TM 1517	*P. robustus*	600–650	25
OH 7	*H. habilis*	729–824	69
KNM-ER 1813	*H. habilis*	510	66
OH 16	*H. habilis*	638	25
OH 24	*H. habilis*	590–594	25
KNM-ER 1470	*H. rudolfensis*	752	66
D2280	*H. erectus* s.l.	730	66
D2282	*H. erectus* s.l.	650	66
D3444	*H. erectus* s.l.	641	66
BOU-VP-2/66	*H. erectus* s.l.	995	25
Bukuran	*H. erectus* s.l.	916	25
KNM-ER 3732	*H. erectus* s.l.	700–775	25
KNM-ER 3733	*H. erectus* s.l.	715–848	25
KNM-ER 3883	*H. erectus* s.l.	785–804	25
Lantian	*H. erectus* s.l.	780	25
Nanjing 1	*H. erectus* s.l.	871–876	25
OH 12	*H. erectus* s.l.	656–727	25
Sangiran 10	*H. erectus* s.l.	839–975	25

Sangiran 12	*H. erectus* s.l.	900–1059	25
Sangiran 17	*H. erectus* s.l.	960–1004	25
Tjg-1993.05	*H. erectus* s.l.	845–870	25
UA 31	*H. erectus* s.l.	995	25
Yunxian	*H. erectus* s.l.	1150	25
Zhoukoudian II	*H. erectus* s.l.	995–1030	25
Zhoukoudian III	*H. erectus* s.l.	915	25
Zhoukoudian V	*H. erectus* s.l.	1300	25
Zhoukoudian VI	*H. erectus* s.l.	850	25
Zhoukoudian X	*H. erectus* s.l.	1225–1245	25
Zhoukoudian XI	*H. erectus* s.l.	1015–1020	25
Zhoukoudian XII	*H. erectus* s.l.	1020–1030	25
Atapuerca 5	Middle Pleistocene *Homo*	1125	70
Atapuerca 4	Middle Pleistocene *Homo*	1390	70
Bodo 1	Middle Pleistocene *Homo*	1250	70
Kabwe 1	Middle Pleistocene *Homo*	1280	70
Petralona	Middle Pleistocene *Homo*	1230	70
LB1	*H. floresiensis*	417	71
DH1–DH2	Rising Star	560	1
DH3–DH4	Rising Star	465	1
LES1	Rising Star	610	2

Supplementary Table S3. List of the fossil material included in the comparison of the postorbital constriction index.

Specimen	Species/group	Postorbital constriction index	Reference
MRD-VP-1/1	*A. anamensis*	62.8	65
A.L. 444-2	*A. afarensis*	64.7	65,72
Sts 5	*A. africanus*	68.1	65
Sts 71	*A. africanus*	60.9	65
StW 505	*A. africanus*	67.0	8
MH1	*A. sediba*	81.4	8
SK 48	*P. robustus*	66.4	73
DNH7	*P. robustus*	84.2	41
OH 5	*P. boisei*	56.5	73
KNM-ER 406	*P. boisei*	53.9	73
KNM-ER 732	*P. boisei*	67.8	73
KNM-WT 17000	*P. aethiopicus*	59.0	73,74
KNM-ER 1470	*H. rudolfensis*	73.6	8
KNM-ER 1813	*H. habilis*	69.0	73
KNM-ER 3733	*H. erectus* s.l.	75.6	8
KNM-ER 3883	*H. erectus* s.l.	73.3	8
D2280	*H. erectus* s.l.	80.0	8
D2282	*H. erectus* s.l.	89.7	8
BOU-VP-2/66	*H. erectus* s.l.	76.6	8
SK 847	*H. erectus* s.l.	82.7	8
Sangiran 2	*H. erectus* s.l.	81.4	66,75
Sangiran 17	*H. erectus* s.l.	80.8	76
Zhoukoudian EI	*H. erectus* s.l.	82.2	8
Zhoukoudian LI	*H. erectus* s.l.	87.5	8
Zhoukoudian LII	*H. erectus* s.l.	78.8	8
Bodo	Middle Pleistocene *Homo*	79.1	8
Kabwe 1	Middle Pleistocene *Homo*	83.7	8
Petralona	Middle Pleistocene *Homo*	81.8	8
Arago	Middle Pleistocene *Homo*	84.6	8
Singa	Middle Pleistocene *Homo*	82.5	8
LB1	*H. floresiensis*	69.3	77
DH3	Rising Star	79.1	1

Supplementary Table S4. List of the fossil material included in the comparison of the postorbital breadth/biparietal breadth index.

Specimen	Species/group	Postorbital breadth/biparietal breadth index	Reference
MRD-VP-1/1	*A. anamensis*	74.5	65
A.L. 444-2	*A. afarensis*	63.1	65,72,78
Sts 5	*A. africanus*	67.3	8
Sts 71	*A. africanus*	68.5	8
MH1	*A. sediba*	73.0	38
SK 48	*P. robustus*	71.0	73,78
OH 5	*P. boisei*	59.1	30,73
KNM-ER 406	*P. boisei*	59.6	30,73
KNM-ER 732	*P. boisei*	67.8	30,73
KNM-WT 17000	*P. aethiopicus*	62.0	73,78
KNM-ER 1470	*H. rudolfensis*	65.0	8
KNM-ER 1813	*H. habilis*	70.4	30,73
D2280	*H. erectus* s.l.	70.6	8
D2282	*H. erectus* s.l.	67.2	8
BOU-VP-2/66	*H. erectus* s.l.	73.1	8
KNM-ER 3733	*H. erectus* s.l.	70.9	8
KNM-ER 3883	*H. erectus* s.l.	66.7	8
Sangiran 2	*H. erectus* s.l.	61.0	8
Sangiran 17	*H. erectus* s.l.	70.1	8
Trinil II	*H. erectus* s.l.	72.2	8
Zhoukoudian EI	*H. erectus* s.l.	72.2	8
Zhoukoudian LI	*H. erectus* s.l.	71.0	8
Zhoukoudian LII	*H. erectus* s.l.	68.9	8
Zhoukoudian LIII	*H. erectus* s.l.	68.3	8
Arago	Middle Pleistocene *Homo*	90.4	8
Bodo	Middle Pleistocene *Homo*	72.8	8
Kabwe 1	Middle Pleistocene *Homo*	70.5	8
Atapuerca H5	Middle Pleistocene *Homo*	73.1	8
Petralona	Middle Pleistocene *Homo*	72.0	8
Singa	Middle Pleistocene *Homo*	67.1	8
LB1	*H. floresiensis*	64.5	77
DH3	Rising Star	66.0	1

Supplementary Table S5. List of the fossil material included in the comparison of the origin of the zygomatic process.

Specimen	Species/group	Origin of zygomatic process	Reference
MRD-VP-1/1	*A. anamensis*	M^1	65
A.L. 444-2	*A. afarensis*	M^1	79
MH 1	*A. sediba*	P^4–M^1	79
Sts 5	*A. africanus*	M^1	This study
Sts 71	*A. africanus*	M^1	79
StW 53	*A. africanus*	M^1	79
KNM-WT 17000	*P. aethiopicus*	P^4–M^1	79
KNM-ER 406	*P. boisei*	P^4	79
OH 5	*P. boisei*	P^4	79
SK 12	*P. robustus*	P^3–P^4	79
SK 13	*P. robustus*	P^3–P^4	41
SK 46	*P. robustus*	P^3–P^4	41
SK 48	*P. robustus*	P^4	This study
SKW 11	*P. robustus*	P^4–M^1	41
DNH 7	*P. robustus*	P^4	41
KNM-ER 1813	*H. habilis*	P^4–M^1	79
OH 24	*H. habilis*	P^4–M^1	This study
KNM-ER 1470	*H. rudolfensis*	P^4	This study
KNM-ER 3733	*H. erectus* s.l.	M^1–M^2	This study
Arago 21	Middle Pleistocene *Homo*	M^1	79
Atapuerca H5	Middle Pleistocene *Homo*	M^1	79
Kabwe 1	Middle Pleistocene *Homo*	M^2	79
Petralona 1	Middle Pleistocene *Homo*	M^1–M^2	This study
LB1	*H. floresiensis*	M^1	77
DNH1	Rising Star	P^3–P^4	1

Supplementary Table S6. List of the fossil material included in the comparison of the index of palate protrusion.

Specimen	Species/group	Index of palate protrusion	Reference
AL 444-2	*A. afarensis*	55	73
AL 417-1d	*A. afarensis*	59	73
Sts 5	*A. africanus*	68	73
Sts 52a	*A. africanus*	52	73
Sts 71	*A. africanus*	47	80
StW 53	*A. africanus*	47	80
MH1	*A. sediba*	43	80
KNM-WT 17000	*P. aethiopicus*	82	73
OH 5	*P. boisei*	43	73
KM-ER 406	*P. boisei*	53	73
KM-ER 732	*P. boisei*	41	73
DNH 155	*P. robustus*	60	81
SK 48	*P. robustus*	46	73
KNM-ER 1813	*H. habilis*	42	80
OH 24	*H. habilis*	48	80
D2700/2735	*H. erectus* s.l.	29	80
KNM-ER 3733	*H. erectus* s.l.	26	80
SK 847	*H. erectus* s.l.	31	80
Kabwe	Middle Pleistocene *Homo*	32	This study
Irhoud 1	Middle Pleistocene *Homo*	36	This study
Atapuerca Cr-5	Middle Pleistocene *Homo*	30	This study
Atapuerca Cr-15	Middle Pleistocene *Homo*	35	This study
Atapuerca Cr-17	Middle Pleistocene *Homo*	31	This study
LB1	*H. floresiensis*	37	77; This study
LES1	Rising Star	50	This study

Supplementary Table S7. List of the fossil material included in the comparison of the index of maxilloalveolar length/breadth.

Specimen	Species/group	Maxilloalveolar length/breadth	Reference
A.L. 200-1a	*A. afarensis*	111	30
A.L. 333-105	*A. afarensis*	102	30
Sts 5	*A. africanus*	112	8
Sts 17	*A. africanus*	105	8
Sts 52	*A. africanus*	100	8
Sts 53	*A. africanus*	106	8
Sts 71	*A. africanus*	106	30
Stw 73	*A. africanus*	107	8
MH1	*A. sediba*	100	8
KNM-ER 405	*P. boisei*	95	30
KNM-ER 406	*P. boisei*	101	30
OH 5	*P. boisei*	105	30
SK 11	*P. robustus*	93	30
SK 13/14	*P. robustus*	106	30
SK 46	*P. robustus*	99	30
SK 48	*P. robustus*	111	30
SK 79	*P. robustus*	100	30
SK 83	*P. robustus*	99	30
KNM-ER 1813	*H. habilis*	94	8
OH 24	*H. habilis*	91	30
D2282	*H. erectus* s.l.	102	8
D2700	*H. erectus* s.l.	95	8
KNM-ER 3733	*H. erectus* s.l.	95	8
Sangiran 4	*H. erectus* s.l.	96	8
SK 847	*H. erectus* s.l.	98	30
Zhoukoudian	*H. erectus* s.l.	90	30
Arago	Middle Pleistocene *Homo*	90	8
Bodo	Middle Pleistocene *Homo*	94	8
Kabwe	Middle Pleistocene *Homo*	90	8
Petralona	Middle Pleistocene *Homo*	85	8
LB1	*H. floresiensis*	84	77
DH1	Rising Star	93	8

Supplementary Table S8. List of the fossil material included in the comparison of the corpus shape index at M_1 level.

Specimen	Species/group	Corpus shape index	Reference
A.L. 228-2	*A. afarensis*	51.3	73
A.L. 315-22	*A. afarensis*	64.6	73
A.L. 330-5	*A. afarensis*	67.2	73
A.L. 417-1a	*A. afarensis*	50.0	73
A.L. 433-1a, b	*A. afarensis*	57.7	73
A.L. 437-1	*A. afarensis*	50.0	73
A.L. 437-2	*A. afarensis*	57.7	73
A.L. 438-1	*A. afarensis*	59.8	73
A.L. 444-2	*A. afarensis*	55.8	73
A.L. 620-1	*A. afarensis*	56.6	73
A.L. 198-1	*A. afarensis*	50.8	73
A.L. 207-13	*A. afarensis*	63.7	73
A.L. 266-1	*A. afarensis*	68.9	73
A.L. 277-1	*A. afarensis*	48.4	73
A.L. 288-1i	*A. afarensis*	57.0	73
A.L. 333w-1a, b	*A. afarensis*	55.0	73
A.L. 333w-12	*A. afarensis*	56.9	73
A.L. 333w-32+60	*A. afarensis*	61.5	73
A.L. 400-1a	*A. afarensis*	52.8	73
MAK-VP 1/12	*A. afarensis*	61.3	73
LH 4	*A. afarensis*	61.8	73
MH1	*A. sediba*	64.3	38
MH2	*A. sediba*	54.8	8
MLD 18	*A. africanus*	61.8	8
MLD 29	*A. africanus*	62.2	8
MLD 34	*A. africanus*	62.5	8
MLD 40	*A. africanus*	65.3	82
Sts 7	*A. africanus*	57.8	82
Sts 36	*A. africanus*	55.6	82
Sts 52	*A. africanus*	83.1	82
KNM-ER 3229	*P. boisei*	71.8	30
KNM-ER 3230	*P. boisei*	69.0	30
KNM-ER 3729	*P. boisei*	73.7	30
KNM-ER 3732	*P. boisei*	60.0	30

KNM-ER 3954	*P. boisei*	76.5	30
KNM-ER 5429	*P. boisei*	68.2	30
KNM-ER 5877	*P. boisei*	65.9	30
KNM-ER 15930	*P. boisei*	71.4	30
KNM-ER 16841	*P. boisei*	63.5	30
OMO L7A-125	*P. boisei*	71.1	30
OMO L74A-21	*P. boisei*	57.5	30
OMO L860-2	*P. boisei*	60.6	30
OMO 18.18	*P. boisei*	74.3	30
Peninj 1	*P. boisei*	73.0	30
SK 6	*P. robustus*	64.0	30
SK 12	*P. robustus*	74.4	30
SK 23	*P. robustus*	64.5	30
SK 34	*P. robustus*	55.6	30
TM 1517	*P. robustus*	68.6	30
DNH 7	*P. robustus*	72.9	41
DNH 8	*P. robustus*	69.4	41
OH 37	*H. habilis*	60.9	30
KNM-ER 1502	*H. habilis*	63.0	30
KNM-ER 1801	*H. habilis*	58.8	30
KNM-ER 1802	*H. habilis*	60.5	30
SK 45	*H. erectus* s.l.	40.5	8
OH 22	*H. erectus* s.l.	63.6	8
KGA 10-1	*H. erectus* s.l.	68.8	8
KNM-ER 730	*H. erectus* s.l.	60.3	30
KNM-ER 992	*H. erectus* s.l.	63.5	30
Sangiran 1b	*H. erectus* s.l.	45.8	30
Tighenif 1	*H. erectus* s.l.	52.8	30
Tighenif 2	*H. erectus* s.l.	48.6	30
Tighenif 3	*H. erectus* s.l.	50.0	30
ZH FI	*H. erectus* s.l.	57.7	8
ZH GI	*H. erectus* s.l.	54.5	8
Zh H1	*H. erectus* s.l.	60.0	8
Zh K1	*H. erectus* s.l.	69.2	8
Zh AN16	*H. erectus* s.l.	59.0	8
Zh Pa86	*H. erectus* s.l.	59.3	8
ATD6-96	Middle–Late Pleistocene *Homo*	58.2	83

ATD6-5	Middle–Late Pleistocene *Homo*	61.0	83
ATD6-113	Middle–Late Pleistocene *Homo*	61.3	83
Arago 2	Middle–Late Pleistocene *Homo*	71.0	8
Arago 13	Middle–Late Pleistocene *Homo*	60.6	8
LB1	Middle–Late Pleistocene *Homo*	73.2	84
LB6	Middle–Late Pleistocene *Homo*	62.2	84
DH1	Rising Star	61.5	2
DH3	Rising Star	57.1	2
101-001	Rising Star	51.7	2
101-377	Rising Star	80.0	2
101-1142	Rising Star	59.3	2

Supplementary Table S9. List of the fossil material included in the comparison of the P_3 root configuration.

specimen	taxon	root configuration[a]	Reference
NFR-VP-1/29	*A. afarensis*	2R: MB + D	85
MLD 18	*A. africanus*	2R: MB + D	86
MLD 27	*A. africanus*	2-D-1	86
MLD 40	*A. africanus*	2R: MB + D	86
Sts 7	*A. africanus*	2R: MB + D	86
Sts 36	*A. africanus*	2-D-1	86
Sts 52b	*A. africanus*	2R: MB + D	86
StW 7	*A. africanus*	2-D-1	86
StW 39	*A. africanus*	2R: MB + D	86
StW 95	*A. africanus*	2-D-1	86
StW 142	*A. africanus*	2R: M + D	86
StW 212 (StW 240)	*A. africanus*	2R: M + D	86
StW 289	*A. africanus*	2-D-1	86
StW 401	*A. africanus*	2R: M + D	86
StW 404	*A. africanus*	2R: M + D	86
StW 498d	*A. africanus*	2R: M + D	86
KNM-ER 403	*P. boisei*	2R: MB + D	87
KNM-ER 725	*P. boisei*	2R: MB + D	87
KNM-ER 726	*P. boisei*	2R: MB + D	87
KNM-ER 733	*P. boisei*	2R: MB + D	87
KNM-ER 3729	*P. boisei*	2R: MB + D	87
KNM-ER 810	*P. boisei*	2R: M + D	87
KNM-ER 3229	*P. boisei*	2R: M + D	87
KNM-ER 3731	*P. boisei*	2R: M + D	87
KNM-ER 3954	*P. boisei*	2R: M + D	87
Peninj	*P. boisei*	2R: M + D	87
DNH 8	*P. robustus*	2R: M + D	86
DNH 58	*P. robustus*	1R	86
DNH 68	*P. robustus*	2R: MB + D	86
SK 6	*P. robustus*	2R: MB + D	86
SK 23	*P. robustus*	2R: M + D	86
SK 30	*P. robustus*	2R: MB + D	86
SK 55b	*P. robustus*	2R: M + D	86
SK 72	*P. robustus*	2R: M + D	86

SK 74a	*P. robustus*	2R: MB + D	86
SK 81	*P. robustus*	2R: MB + D	86
SK 857	*P. robustus*	2R: MB + D	86
SK 858.861.883	*P. robustus*	2R: M + D	86
SK 876	*P. robustus*	2R: M + D	86
SK 1587a	*P. robustus*	3-C-1	86
SK 1588	*P. robustus*	2R: M + D	86
SKW 5	*P. robustus*	2R: M + D	86
SKX 311	*P. robustus*	2T	86
SKX 4446	*P. robustus*	2R: M + D	86
TM 1517	*P. robustus*	2R: M + D	86
OH 7	*H. habilis*	2T	87
OH 13	*H. habilis*	1R	87
OH 16	*H. habilis*	1R	87
OH 23	*H. habilis*	1R	87
KNM-ER 1801	*H. habilis*	2T	87
KNM-ER 1802	*H. habilis*	2R: M + D	87
KNM-ER 1806	*H. habilis*	2R: M + D	87
KNM-ER 1483	*H. rudolfensis*?	1R	87
KNM-ER 730	*H. erectus* s.l.	2R: MB + D	87
D2600	*H. erectus* s.l.	2R: MB + D	3
KNM-ER 992	*H. erectus* s.l.	2T	87
KNM-ER 1812	*H. erectus* s.l.	1R	87
OH 22	*H. erectus* s.l.	1R	87
OH 37	*H. erectus* s.l.	1R	87
Sangiran 1b	*H. erectus* s.l.	1R	This study (based on root socket)
PA110	*H. erectus* s.l.	1R	88
PA526	*H. erectus* s.l.	2T	88
PA527	*H. erectus* s.l.	2T	88
PA102	*H. erectus* s.l.	2T	88
ATD6-3	*H. antecessor*	2R: M + D	89
PA1578	Middle Pleistocene *Homo*	1R	88
Atapuerca SH (n = 36)	Middle Pleistocene *Homo*	1R	90
LB1	*H. floresiensis*	2R: MB + D	84
LB2	*H. floresiensis*	1R	84
LB6	*H. floresiensis*	2R: MB + D	84
U.W. 101-144	Rising Star	2R: MB + D	3

U.W. 101-358	Rising Star	2R: MB + D	3
U.W. 101-506	Rising Star	2R: MB + D	3
U.W. 101-800	Rising Star	2R: MB + D	3
U.W. 101-001+U.W. 101-850	Rising Star	2R: MB + D	3
U.W. 101-1261 (n = 2)	Rising Star	2R: MB + D	3

[a] Categories from Ref. 86 are not identical to those originally developed by Ref. 87. Since most data on P_3 roots available to date are still those from Ref. 30, Ref. 90's categories were converted back into the originally proposed format as follows: 1-A-1 = 1R; 2-A-3 = 2T; 2-B-1 and 3-A-1 = 2R: MB + D; 2-C-1, 3-B-1 and 4-A-1 = 2R: M + D. The other categories of Ref. 86, not coded in the hominins investigated by Ref. 87, were not converted.

Supplementary Table S10. List of the fossil material included in the comparison of the buccally-deflected M_3 distal root.

Specimen	Species/group	buccally-deflected M_3 root	Reference
GLL 33	*A.* cf. *afarensis*	present	91
StW 212	*A. africanus*	absent	This study
StW 353	*A. africanus*	present	This study
StW 384	*A. africanus*	absent	This study
StW 404	*A. africanus*	present	29; this study
StW 498c	*A. africanus*	absent	29
StW 531	*A. africanus*	absent	This study
KNM-ER 15930	*P. boisei*	absent	29
KNM-ER 729	*P. boisei*	present	29
SK 22	*P. robustus*	present	This study
SK 23	*P. robustus*	present	29
SK 34	*P. robustus*	present	This study
SK 840	*P. robustus*	absent	This study
SK 858	*P. robustus*	present	This study
SK 880	*P. robustus*	present	This study
SK 1586	*P. robustus*	present	29
SKX 5014	*P. robustus*	present	This study
DNH 18	*P. robustus*	present	This study
DNH 21	*P. robustus*	present	This study
DNH 68	*P. robustus*	present	This study
OH 4	*H. habilis*	absent	This study
KNM-ER 730	*H. erectus* s.l.	absent	29
KNM-ER 992	*H. erectus* s.l.	absent	29
SK 45	*H. erectus* s.l.	absent	This study (based on the alveolar socket)
Sangiran 1b	*H. erectus* s.l.	absent	This study
PA834-2	*H. erectus* s.l.	absent	92
BH1	Middle Pleistocene *Homo*	absent	29
Mauer	Middle Pleistocene *Homo*	absent	29
U.W. 101-001	Rising Star hominins	present	29
U.W. 101-1261	Rising Star hominins	present	29
U.W. 101-1142	Rising Star hominins	present	29
U.W. 101-361	Rising Star hominins	present	29
U.W. 101-516	Rising Star hominins	present	29

Supplementary Table S11. List of the fossil material included in the geometric morphometric analyses of the neurocranium shape in lateral and posterior views.

Specimen	Analysis	Group	Reference
MRD-VP-1.1	lateral and posterior views	*Australopithecus*	65
A.L. 333-45	posterior view	*Australopithecus*	65
A.L. 444-2	lateral and posterior views	*Australopithecus*	65
A.L. 822-2	lateral view	*Australopithecus*	65
MLD 37.38	posterior view	*Australopithecus*	65
Sts 5	lateral and posterior views	*Australopithecus*	65; this study
Sts 71	lateral view	*Australopithecus*	93
StW 53	posterior view	*Australopithecus*	94
StW 505	lateral view	*Australopithecus*	93
StW 573	posterior view	*Australopithecus*	94
KNM-WT 17000	lateral and posterior views	*Paranthropus*	95
KNM-WT 17400	posterior view	*Paranthropus*	https://africanfossils.org
KNM-ER 406	lateral and posterior views	*Paranthropus*	96; https://africanfossils.org
KNM-ER 13750	lateral view	*Paranthropus*	95
KNM-ER 23000	lateral and posterior views	*Paranthropus*	97
OH 5	Lateral and posterior view	*Paranthropus*	98; this study
DNH 7	lateral and posterior views	*Paranthropus*	41; Morphosource.org
DNH 155	lateral view	*Paranthropus*	81
SK 46	lateral view	*Paranthropus*	93
KNM-ER 1470	lateral and posterior views	*Homo*	2; https://africanfossils.org
KNM-ER 1813	lateral and posterior views	*Homo*	99
KNM-ER 3733	lateral and posterior views	*Homo*	100
D2282	lateral and posterior views	*Homo*	66
D2280	lateral and posterior views	*Homo*	66
D3444	lateral and posterior views	*Homo*	66
Sangiran 2	lateral and posterior views	*Homo*	100,101
Sangiran 4	posterior view	*Homo*	101
Sangiran 12	posterior view	*Homo*	101
Sangiran 17	lateral and posterior views	*Homo*	102; this study
Tjg-1993.05	lateral and posterior views	*Homo*	103
Trinil	posterior view	*Homo*	101
Zhoukoudian	lateral and posterior views	*Homo*	this study
Hexian	lateral and posterior views	*Homo*	104,105
Kabwe 1	lateral and posterior views	*Homo*	106

Irhoud 1	lateral view	*Homo*	107
LB1	lateral and posterior views	*Homo*	77
DH1	lateral and posterior views	Rising Star	1; http://www.morphosource.org
LES1	lateral view	Rising Star	2

Supplementary Table S12. List of the fossil material included in the geometric morphometric analyses of the maxilla profile.

Specimen	Group	Reference
A.L. 417-1	*Australopithecus*	65
A.L. 200-1	*Australopithecus*	65
TM 1511	*Australopithecus*	This study
MRD-VT-1/1	*Australopithecus*	65
StW 573	*Australopithecus*	94
StW 53	*Australopithecus*	108
StW 13	*Australopithecus*	This study
StW 505	*Australopithecus*	This study
Sts 71	*Australopithecus*	93
A.L. 444-2	*Australopithecus*	65
A.L. 822-2	*Australopithecus*	109
DNH 155	*Paranthropus*	81
DNH 7	*Paranthropus*	41
SK 46	*Paranthropus*	93
OH 5	*Paranthropus*	This study
KNM-ER 732	*Paranthropus*	96
SK 12a	*Paranthropus*	This study
SK 11	*Paranthropus*	This study
SK 13-14	*Paranthropus*	This study
SK 83	*Paranthropus*	This study
SK 43-SKW 7	*Paranthropus*	This study
SK 52	*Paranthropus*	This study
SK 79	*Paranthropus*	This study
Sangiran 17	*Homo*	102
SK 847	*Homo*	This study
Sangiran 4	*Homo*	This study
KNM-ER 1813	*Homo*	99
KNM-ER 3384	*Homo*	56
Tjg-1993.05	*Homo*	103
OH 65	*Homo*	110
KNM-ER 3733	*Homo*	101
Bpg 2001.04	*Homo*	111
Zhoukoudian	*Homo*	This study
D2282	*Homo*	66
D4500	*Homo*	66
Kabwe 1	*Homo*	106
Irhoud 1	*Homo*	107
LB1	*Homo*	77
DH1	Rising Star	1; http://www.morphosource.org

Supplementary Table S13. List of the fossil material included in the geometric morphometric analyses of the M_2 enamel-dentine junction.

Specimen	Group	Reference
A.L. 333w-1a	*Australopithecus*	42
A.L. 333w-57	*Australopithecus*	42
A.L. 188-1	*Australopithecus*	42
A.L. 330-5	*Australopithecus*	42
A.L. 400-1a	*Australopithecus*	42
A.L. 417-1a	*Australopithecus*	42
A.L. 440-1	*Australopithecus*	42
A.L. 443-1ac	*Australopithecus*	42
A.L. 128-23	*Australopithecus*	42
A.L. 145-35	*Australopithecus*	42
A.L. 241-14	*Australopithecus*	42
MLD 2 L	*Australopithecus*	42
MLD 2 R	*Australopithecus*	42
Sts 52 L	*Australopithecus*	42
Sts 52 R	*Australopithecus*	42
StW 3	*Australopithecus*	42
StW 14	*Australopithecus*	42
StW 61	*Australopithecus*	42
StW 109	*Australopithecus*	42
StW 120	*Australopithecus*	42
StW 133	*Australopithecus*	42
StW 213	*Australopithecus*	42
StW 234	*Australopithecus*	42
StW 295	*Australopithecus*	42
StW 322	*Australopithecus*	42
StW 327	*Australopithecus*	42
StW 384	*Australopithecus*	42
StW 404	*Australopithecus*	42
StW 498	*Australopithecus*	42
StW 519	*Australopithecus*	42
StW 520	*Australopithecus*	42
StW 534	*Australopithecus*	42
StW 560d	*Australopithecus*	42
StW 560e	*Australopithecus*	42
OH 7	*Homo*	42
KNM-ER 1802	*Homo*	42
CA 808	*Homo*	42
KNM-ER 992 L	*Homo*	42
KNM-ER 992 R	*Homo*	42
MA 93	*Homo*	42
PA70	*Homo*	42

PA533	*Homo*	42
Sangiran 1b	*Homo*	42
Sangiran 7-20	*Homo*	42
Sangiran 7-64	*Homo*	42
Sangiran 7-65	*Homo*	42
SMF-8865	*Homo*	42
Tighenif 2	*Homo*	42
KNM-ER 3230 L	*Paranthropus*	42
KNM-ER 3230 R	*Paranthropus*	42
KNM-ER 6080	*Paranthropus*	42
KNM-ER 15930	*Paranthropus*	42
KNM-ER 15940	*Paranthropus*	42
KNM-ER 25520	*Paranthropus*	42
DNH 7 L	*Paranthropus*	42
DNH 7 R	*Paranthropus*	42
DNH 8 L	*Paranthropus*	42
DNH 21	*Paranthropus*	42
DNH 51	*Paranthropus*	42
DNH 60	*Paranthropus*	42
DNH 68	*Paranthropus*	42
SK 1	*Paranthropus*	42
SK 6 L	*Paranthropus*	42
SK 6 R	*Paranthropus*	42
SK 23 L	*Paranthropus*	42
SK 23 R	*Paranthropus*	42
SK 25 L	*Paranthropus*	42
SK 34	*Paranthropus*	42
SK 843	*Paranthropus*	42
SK 858 R	*Paranthropus*	42
SK 1587a	*Paranthropus*	42
SK 1587b	*Paranthropus*	42
SK 3976	*Paranthropus*	42
SKW 5 L	*Paranthropus*	42
SKX 4446	*Paranthropus*	42
TM 1600	*Paranthropus*	42
U.W. 101-377	Rising Star	This study

Supplementary Table S14. List of the fossil material included in the analysis of the canine to M_3 ratio of the square root of crown area.

Specimen	Tooth	Group/species	Root of crown area	References
Sts 36	C_1	*A. africanus*	10.14	30
Sts 50	C_1	*A. africanus*	9.64	30
Sts 51	C_1	*A. africanus*	8.84	30
Sts 52b	C_1	*A. africanus*	9.54	30
StW 21	C_1	*A. africanus*	9.90	113
StW 58	C_1	*A. africanus*	9.74	113
Stw 110	C_1	*A. africanus*	9.93	113
StW 116	C_1	*A. africanus*	10.68	113
StW 132	C_1	*A. africanus*	9.79	113
StW 142	C_1	*A. africanus*	9.18	113
StW 143	C_1	*A. africanus*	9.85	113
StW 151	C_1	*A. africanus*	8.35	113
StW 213	C_1	*A. africanus*	8.65	113
StW 288	C_1	*A. africanus*	10.32	113
StW 351	C_1	*A. africanus*	9.74	113
StW 365	C_1	*A. africanus*	10.40	113
StW 446	C_1	*A. africanus*	8.95	113
StW 476	C_1	*A. africanus*	9.60	113
StW 491	C_1	*A. africanus*	9.45	113
StW 491	C_1	*A. africanus*	9.74	113
StW 537	C_1	*A. africanus*	10.28	113
StW 537	C_1	*A. africanus*	10.38	113
KNM-ER 729G	C_1	*P. boisei*	9.13	30
KNM-ER 1477D	C_1	*P. boisei*	7.55	30
KNM-ER 3230	C_1	*P. boisei*	8.47	30
KNM-ER 3230	C_1	*P. boisei*	8.44	30
OH 30	C_1	*P. boisei*	7.75	114
Peninj 1	C_1	*P. boisei*	7.69	114
Peninj 1	C_1	*P. boisei*	7.84	114
SK 23	C_1	*P. robustus*	8.00	30
SK 23	C_1	*P. robustus*	7.50	30
SK 29	C_1	*P. robustus*	7.95	30
SK 34	C_1	*P. robustus*	8.75	30
SK 63	C_1	*P. robustus*	7.40	30
SK 87	C_1	*P. robustus*	8.47	30
SK 94	C_1	*P. robustus*	8.15	30
SK 820	C_1	*P. robustus*	7.20	30
SKX 241	C_1	*P. robustus*	7.25	30
SKX 5007	C_1	*P. robustus*	7.84	30

SKX 6013	C_1	*P. robustus*	7.29	30
DNH 8	C_1	*P. robustus*	8.30	130
DNH 8	C_1	*P. robustus*	8.44	130
DNH 79	C_1	*P. robustus*	7.93	130
DNH 77b	C_1	*P. robustus*	7.50	116
DNH 79b	C_1	*P. robustus*	7.88	116
DNH 91	C_1	*P. robustus*	7.35	116
OH 7	C_1	*H. habilis*	9.43	114
OH 13	C_1	*H. habilis*	8.10	114
D211	C_1	Dmanisi	8.45	117
D211	C_1	Dmanisi	8.35	117
D2735	C_1	Dmanisi	9.55	117
D2735	C_1	Dmanisi	9.45	117
D2600	C_1	Dmanisi	8.83	117
D2600	C_1	Dmanisi	9.32	117
KNM-ER 992	C_1	*H. erectus* s.l.	9.20	30
Tighenif 3	C_1	*H. erectus* s.l.	9.08	30
ZKD B5-77	C_1	*H. erectus* s.l.	9.53	30
ZKD C2-29	C_1	*H. erectus* s.l.	9.67	30
ZKD C4-52	C_1	*H. erectus* s.l.	8.60	30
ZKD G1-6	C_1	*H. erectus* s.l.	8.15	30
ZKD H4-83	C_1	*H. erectus* s.l.	9.10	30
LB1	C_1	*H. floresiensis*	7.04	118
LB6	C_1	*H. floresiensis*	6.45	118
LES1	C_1	Rising Star	7.39	2
LES1	C_1	Rising Star	7.65	2
U.W. 102b-511	C_1	Rising Star	6.80	2
U.W. 101-339	C_1	Rising Star	7.20	3
U.W. 101-886	C_1	Rising Star	7.10	3
U.W. 101-985	C_1	Rising Star	7.25	3
U.W. 101-1014	C_1	Rising Star	6.80	3
U.W. 101-1076	C_1	Rising Star	7.15	3
U.W. 101-1126	C_1	Rising Star	7.15	3
U.W. 101-1261	C_1	Rising Star	7.05	3
U.W. 101-1261	C_1	Rising Star	7.10	3
StW 14	M_3	*A. africanus*	16.12	113
StW 47	M_3	*A. africanus*	14.98	113
StW 90	M_3	*A. africanus*	15.50	113
StW 109	M_3	*A. africanus*	16.48	113
StW 133	M_3	*A. africanus*	15.73	113
StW 142	M_3	*A. africanus*	15.89	113
StW 212	M_3	*A. africanus*	15.24	113
StW 237	M_3	*A. africanus*	16.92	113

StW 280	M_3	*A. africanus*	16.60	113
StW 295	M_3	*A. africanus*	14.75	113
StW 295	M_3	*A. africanus*	14.79	113
StW 353	M_3	*A. africanus*	12.83	113
StW 384	M_3	*A. africanus*	17.49	113
StW 385	M_3	*A. africanus*	15.39	113
StW 404	M_3	*A. africanus*	14.45	113
StW 487	M_3	*A. africanus*	16.22	113
StW 491	M_3	*A. africanus*	14.87	113
StW 498	M_3	*A. africanus*	17.26	113
StW 520	M_3	*A. africanus*	15.22	113
StW 529	M_3	*A. africanus*	14.59	113
StW 529	M_3	*A. africanus*	14.90	113
StW 537	M_3	*A. africanus*	16.35	113
StW 560	M_3	*A. africanus*	16.54	113
StW 560	M_3	*A. africanus*	16.63	113
KNM-ER 729A	M_3	*P. boisei*	20.31	30
KNM-ER 802F	M_3	*P. boisei*	17.51	30
KNM-ER 810B	M_3	*P. boisei*	16.67	30
KNM-ER 1467	M_3	*P. boisei*	16.97	30
KNM-ER 1509A	M_3	*P. boisei*	17.74	30
KNM-ER 3230	M_3	*P. boisei*	18.68	30
KNM-ER 15930	M_3	*P. boisei*	16.52	30
KNM-ER 15940	M_3	*P. boisei*	17.15	30
KNM-ER 15940	M_3	*P. boisei*	16.70	30
OMO L7A-125	M_3	*P. boisei*	16.41	30
OMO L338x-39	M_3	*P. boisei*	17.12	30
OMO L398-630	M_3	*P. boisei*	16.13	30
OMO L628-3	M_3	*P. boisei*	17.41	30
OMO 33-9	M_3	*P. boisei*	17.03	30
OMO 136-1	M_3	*P. boisei*	16.71	30
OMO 136-2	M_3	*P. boisei*	15.61	30
OMO F22-1b	M_3	*P. boisei*	19.07	30
Peninj 1	M_3	*P. boisei*	17.20	30
TM 1517	M_3	*P. robustus*	15.31	30
SK 6	M_3	*P. robustus*	17.15	30
SK 12	M_3	*P. robustus*	16.27	30
SK 23	M_3	*P. robustus*	15.36	30
SK 34	M_3	*P. robustus*	17.31	30
SK 75	M_3	*P. robustus*	16.20	30
SK 81	M_3	*P. robustus*	16.05	30
SK 840	M_3	*P. robustus*	14.55	30
SK 841b	M_3	*P. robustus*	14.81	30

SK 843	M_3	*P. robustus*	16.26	30
SK 844	M_3	*P. robustus*	14.97	30
SK 880	M_3	*P. robustus*	16.11	30
SK 885	M_3	*P. robustus*	14.73	30
SK 1586	M_3	*P. robustus*	15.69	30
SKX 5002	M_3	*P. robustus*	15.73	30
SKX 5014	M_3	*P. robustus*	16.06	30
DNH 8	M_3	*P. robustus*	17.59	30
DNH 21	M_3	*P. robustus*	14.00	30
DNH 8	M_3	*P. robustus*	17.07	30
DNH 10	M_3	*P. robustus*	15.19	30
DNH 18	M_3	*P. robustus*	16.43	30
DNH 51	M_3	*P. robustus*	15.37	30
DNH 75	M_3	*P. robustus*	15.23	30
DNH 86	M_3	*P. robustus*	15.63	30
DNH 97	M_3	*P. robustus*	15.34	30
OH 4	M_3	*H. habilis*	14.15	30
OH 13	M_3	*H. habilis*	13.52	30
OH 16	M_3	*H. habilis*	15.11	30
OH 27	M_3	*H. habilis*	14.31	30
KNM-ER 1801	M_3	*H. habilis*	15.75	30
D211	M_3	Dmanisi	10.75	117
D211	M_3	Dmanisi	11.13	117
D2600	M_3	Dmanisi	14.71	117
D2600	M_3	Dmanisi	14.71	117
Sangiran 1b	M_3	*H. erectus* s.l.	13.46	30
ZKD A2-2	M_3	*H. erectus* s.l.	10.00	30
ZKD D1-61	M_3	*H. erectus* s.l.	12.15	30
ZKD F1-25	M_3	*H. erectus* s.l.	11.79	30
ZKD G1-6	M_3	*H. erectus* s.l.	12.15	30
ZKD G1-7	M_3	*H. erectus* s.l.	12.65	30
ZKD H1-12	M_3	*H. erectus* s.l.	10.10	30
ZKD L4-302	M_3	*H. erectus* s.l.	11.71	30
ZKD M1-308	M_3	*H. erectus* s.l.	10.85	30
ZKD M3-305	M_3	*H. erectus* s.l.	10.65	30
Sangiran 21	M_3	*H. erectus* s.l.	11.58	119
Sangiran 22	M_3	*H. erectus* s.l.	12.15	119
Sangiran 22	M_3	*H. erectus* s.l.	11.80	119
KNM-ER 730	M_3	*H. erectus* s.l.	12.55	30
KNM-ER 806A	M_3	*H. erectus* s.l.	13.59	30
KNM-ER 806D	M_3	*H. erectus* s.l.	13.31	30
KNM-ER 992A	M_3	*H. erectus* s.l.	12.64	30
KNM-ER 992B	M_3	*H. erectus* s.l.	12.84	30

LB1	M_3	*H. floresiensis*	10.05	84
LB6	M_3	*H. floresiensis*	9.15	84
U.W. 101-001	M_3	Rising Star	12.92	2
U.W. 101-377	M_3	Rising Star	12.48	2
U.W. 101-516	M_3	Rising Star	12.72	2
U.W. 101-1261	M_3	Rising Star	13.29	2
U.W. 101-1261	M_3	Rising Star	12.69	2
U.W. 101-1261	M_3	Rising Star	12.28	2

Supplementary Table S15. List of the fossil material included in the analysis of the cross-sectional shape of the distal humerus diaphysis.

Specimen	Species/group	Reference
A.L. 288-1 left	*Australopithecus*	120
A.L. 288-1 right	*Australopithecus*	120
StW 38	*Australopithecus*	17
StW 124	*Australopithecus*	17
StW 431	*Australopithecus*	17
OH 80	*Paranthropus*	121
KNM-ER 739	*Paranthropus*	16
KNM-ER 1504	*Paranthropus*	16
KNM-ER 45510	*Paranthropus*	122
KNM-ER 47000B	*Paranthropus*	121
TM 1517	*Paranthropus*	123
SKX 10924	*Paranthropus*	123
SKX 10924	*Paranthropus*	124
DNH 32	*Paranthropus*	125
Gombore I	*Homo*	124
SKX 34805	*Homo*	123
StW 150	*Homo*	17
StW 182	*Homo*	17
D4507	*Homo*	124
SOA-MM9	*Homo*	126
LB1	*Homo*	126
U.W. 101-283	Rising Star	http://www.morphosource.org
U.W. 101-466	Rising Star	http://www.morphosource.org
U.W. 101-1240	Rising Star	http://www.morphosource.org

Supplementary Table S16. List of the fossil material included in the analysis of the cross-sectional shape of the femoral neck.

Specimen	Species/group	Reference
A.L. 288-1	*Australopithecus*	120
A.L. 333-3	*Australopithecus*	11
A.L. 333-95	*Australopithecus*	11
U.W. 88-4	*Australopithecus*	11
SK 82	*Paranthropus*	11
SK 97	*Paranthropus*	11
KNM-ER 738	*Paranthropus*	11
KNM-ER 3728	*Paranthropus*	11
KNM-ER 1472	*Homo*	11
KNM-ER 1481	*Homo*	11
KNM-WT 15000	*Homo*	This study
LB1	*Homo*	23
U.W. 101-002	Rising Star	11
U.W. 101-398	Rising Star	11
U.W. 101-1391	Rising Star	11

Supplementary Table S17. Adjusted Z-scores of the corpus shape index computed for the Rising Star specimens in comparison with various species/groups of *Australopithecus*, *Paranthropus* and *Homo*. The value is considered to be statistically compatible with the comparative group if it is included between -1 and 1 and when the specimen is outside the variation of a group, the value is highlighted in bold.

Rising Star specimens	*A. afarensis*	*A. africanus*	*P. boisei*	*P. robustus*	*H. habilis*	*H. erectus* s.l.	Middle–Late Pleistocene *Homo*
DH1	0.32	-0.11	-0.51	-0.33	0.12	0.25	-0.16
DH3	-0.03	-0.29	-0.84	-0.59	-0.61	0.01	-0.45
U.W. 101-001	-0.47	-0.52	**-1.25**	-0.92	**-1.50**	-0.29	-0.81
U.W. 101-377	**1.80**	0.68	0.88	0.78	**3.17**	**1.27**	**1.07**
U.W. 101-1142	0.14	-0.20	-0.68	-0.47	-0.26	0.13	-0.31

Supplementary References

50. Scolan, H., Santos, F., Tillier, A.-M., Maureille, B. & Quintard, A. Des nouveaux vestiges néanderthaliens à Las Pélénos (Monsempron-Libos, Lot-et-Garonne, France). *Bull. Mém. Soc. Anthropol. Paris* **24**, 69–95 (2012).
51. Copes, L.E. & Kimbel, W.H. Cranial vault thickness in primates: *Homo erectus* does not have uniquely thick vault bones. *J. Hum. Evol*. **90**, 120–134 (2016).
52. Holloway, R.L. et al. Endocast morphology of *Homo naledi* from the Dinaledi Chamber, South Africa. *Proc. Natl. Acad. Sci. USA* **115**, 5738–5743 (2018).
53. Hurst, S.D. et al. The endocast morphology of LES1, *Homo naledi*. *Am. J. Biol. Anthropol*. **184**, e24983 (2024).
54. Ponce de León, M.S. et al. The primitive brain of early *Homo*. *Science* **372**, 165–171 (2021).
55. Antón, S.C.& Middleton, E.R. Making meaning from fragmentary fossils: Early *Homo* in the Early to early Middle Pleistocene. *J. Hum. Evol.* **179**, 103307 (2023).
56. Bräuer, G., Leakey, R.E. & Mbua, E. in *Continuity or Replacement? Controversies in* Homo sapiens *Evolution* (eds. Bräuer, G. & Smith, F.H.) 111–120 (Balkema, 1992).
57. Bermúdez de Castro, J.M. et al. Comparative dental study between *Homo antecessor* and Chinese *Homo erectus*: Nonmetric features and geometric morphometrics. *J. Hum. Evol.* **161**, 103087 (2021).
58. Xing, S., Martinón-Torres, M. & Bermúdez de Castro, J.M. The fossil teeth of the Peking Man. *Sci. Rep*. **8**, 2066 (2018).
59. Zanolli, C. et al. Further analyses of the structural organization of *Homo luzonensis* teeth: Evolutionary implications. *J. Hum. Evol.* **163**, 103124 (2022).
60. Skinner, M.M., Gunz, P., Wood, B.A. & Hublin, J.-J. Enamel-dentine junction (EDJ) morphology distinguishes the lower molars of *Australopithecus africanus* and *Paranthropus robustus*. *J. Hum. Evol*. **55**, 979–988 (2008).
61. Skinner, M.M., Gunz, P., Wood, B.A., Boesch, C. & Hublin, J.-J. Discrimination of extant *Pan* species and subspecies using the enamel-dentine junction morphology of lower molars. *Am. J. Phys. Anthropol.* **140**, 234–243 (2009).
62. Zanolli, C. et al. Evidence for increased hominid diversity in the Early-Middle Pleistocene of Indonesia. *Nat. Ecol. Evol*. **3**, 755–764 (2019).

63. Zanolli, C. et al. A reassessment of the distinctiveness of dryopithecine genera from the Iberian Miocene based on enamel-dentine junction geometric morphometric analyses. *J. Hum. Evol*. **177**, 103326 (2023).
64. Zanolli, C. et al. The phylogenetic signal of the enamel-dentine junction of primate molars. *Am. J. Phys. Anthropol*. **177** (S73), 202 (2022).
65. Haile-Selassie, Y., Melillo, S.M., Vazzana, A., Benazzi, S. & Ryan, T.M. A 3.8-million-year-old hominin cranium from Woranso-Mille, Ethiopia. *Nature* **573**, 214–219 (2019).
66. Lordkipanidze, D. et al. A complete skull from Dmanisi, Georgia, and the evolutionary biology of early *Homo*. *Science* **342**, 326–331 (2013).
67. Falk, D. et al. Early hominid brain evolution: A new look at old endocasts. *J. Hum. Evol*. **38**, 695–717 (2000).
68. Beaudet, A. et al. The endocast of StW 573 ("Little Foot") and hominin brain evolution. *J. Hum. Evol.* **126**, 112–123 (2019).
69. Spoor, F. et al. Reconstructed *Homo habilis* type OH 7 suggests deep-rooted species diversity in early *Homo*. *Nature* **519**, 83–86 (2015).
70. Rightmire, G.P. *Homo erectus* and Middle Pleistocene hominins: Brain size, skull form, and species recognition. *J. Hum. Evol*. **65**, 223–252 (2013).
71. Falk, D. et al. The brain of LB1, *Homo floresiensis*. *Science* **308**, 242–245 (2005).
72. Brunet, M. et al. A new hominid from the Upper Miocene of Chad, Central Africa. *Nature* **418**, 145–151 (2002).
73. Kimbel, W.H., Rak, Y. & Johanson, D.C. *The Skull of* Australopithecus afarensis (Oxford University Press, 2004).
74. Curnoe, D. Cranial variability in East African 'robust' hominis. *Hum. Evol.* **16**, 169–198 (2001).
75. Weidenreich, F. The skull of *Sinanthropus pekinensis*: A comparative study on a primitive hominin skull. *Palaeontol. Sin. D* **10**, 1–485 (1943).
76. Kaifu, Y. et al. Cranial morphology of Javanese *Homo erectus*: New evidence for continuous evolution, specialization, and terminal extinction. *J. Hum. Evol*. **55**, 551–580 (2008).
77. Kaifu, Y. et al. Craniofacial morphology of *Homo floresiensis*: Description, taxonomic affinities, and evolutionary implication. *J. Hum. Evol*. **61**, 644–682 (2011).

78. Pérez-Claros, J.A. & Palmqvist, P. Heterochronies and allometries in the evolution of the hominid cranium: A morphometric approach using classical anthropometric variables. *PeerJ* **10**, e13991 (2022).
79. Weber, G.W. & Krenn, V.A. Zygomatic root position in recent and fossil hominids. *Anat. Rec*. **300**, 160–170 (2017).
80. de Ruiter, A.J. et al. The skull of *Australopithecus sediba*. *PaleoAnthropology* **2018**, 56–155 (2018).
81. Martin, J.M. et al. Drimolen cranium DNH 155 documents microevolution in an early hominin species. *Nat. Ecol. Evol*. **5**, 38–45 (2021).
82. de Ruiter, D.J. et al. Mandibular remains support taxonomic validity of *Australopithecus sediba*. *Science* **340**, 1232997-1–1232997-4 (2013).
83. Bermúdez de Castro, J.M., Martinón-Torres, M., Gómez-Robles, A., Prado, L. & Sarmiento, S. Comparative analysis of the Gran Dolina-TD6 (Spain) and Tighennif (Algeria) hominin mandibles. *Bull. Mém. Soc. Anthropol. Paris* **19**, 149–167 (2007).
84. Brown, P. & Maeda, T. Liang Bua *Homo floresiensis* mandibles and mandibular teeth: A contribution to the comparative morphology of a new hominin species. *J. Hum. Evol*. **57**, 571–596 (2009).
85. Haile-Selassie, Y. et al. Dentognathic remains of *Australopithecus afarensis* from Nefuraytu (Woranso-Mille, Ethiopia): Comparative description, geology, and paleoecological context. *J. Hum. Evol*. **100**, 35–53 (2016).
86. Moore, N.C., Thackeray, J.F., Hublin, J.-J. & Skinner, M.M. Premolar root and canal variation in South African Plio-Pleistocene specimens attributed to *Australopithecus africanus* and *Paranthropus robustus*. *J. Hum. Evol*. **93**, 46–62 (2016).
87. Wood, B.A., Abbott, S.A. & Uytterschaut, H. Analysis of the dental morphology or Plio-Pleistocene hominids IV. Mandibular postcanine root morphology. *J. Anat*. **156**, 107–139 (1988).
88. Pan, L., Dumoncel, J., Mazurier, A. & Zanolli, C. Structural analysis of premolar roots in Middle Pleistocene hominins from China. *J. Hum. Evol*. **136**, 102669 (2019).
89. Martinón-Torres, M. et al. New permanent teeth from Gran Dolina-TD6 (Sierra de Atapuerca). The bearing of *Homo antecessor* on the evolutionary scenario of Early and Middle Pleistocene Europe. *J. Hum. Evol*. **127**, 93–117 (2019).

90. Martinón-Torres, M. Evolución del aparato dental en homínidos: estudio de los dientes humanos del Pleistoceno de la Sierra de Atapuerca (Burgos) (Universidad de Santiago de Compostela, 2006).
91. Macchiarelli, R. et al. Early Pliocene hominid tooth from Galili, Somali Region, Ethiopia. *Coll. Antropol*. **28**, 65–76 (2004).
92. Xing, S. et al. Middle Pleistocene hominin teeth from Longtan cave, Hexian, China. *PLoS One* **9**, e114265 (2014).
93. Beaudet, A. et al. Cranial vault thickness variation and inner structural organization in the StW 578 hominin cranium from Jacovec Cavern, South Africa. *J. Hum. Evol*. **121**, 204–220 (2018).
94. Clarke, R.J. & Kuman, K. The skull of StW 573, a 3.67 Ma *Australopithecus prometheus* skeleton from Sterkfontein Caves, South Africa. *J. Hum. Evol*. **134**, 102634 (2019).
95. Leakey, R.E.F. & Walker, A. New *Australopithecus boisei* specimens from East and West Lake Turkana, Kenya. *Am. J. Phys. Anthropol*. **76**, 1–24 (1988).
96. Wood, B.A. & Constantino, P. *Paranthropus boisei*: Fifty years of evidence and analysis. *Yearb. Phys. Anthropol.* **50**, 106–132 (2007).
97. Brown, B., Walker, A., Ward, C.V. & Leakey, R.E.F. New *Australopithecus boisei* calvaria from East Lake Turkana, Kenya. *Am. J. Phys. Anthropol*. **91**, 137–159 (1993).
98. Benazzi, S., Bookstein, F.L., Strait, D.S. & Weber, G.W. A new OH5 reconstruction with an assessment of its uncertainty. *J. Hum. Evol*. **61**, 75–88 (2011).
99. Benazzi, S., Gruppioni, G., Strait, D.S. & Hublin, J.-J. Technical Note: Virtual reconstruction of KNM-ER 1813 *Homo habilis* cranium. *Am. J. Phys. Anthropol*. **153**, 154–160 (2014).
100. Schwartz, J.H., Tattersall, I. & Chi, Z. Comment on "A complete skull from Dmanisi, Georgia, and the evolutionary biology of early *Homo*". *Science* **344**, 360-a (2014).
101. Schwartz, J.H. Getting to know *Homo erectus*. *Science* **305**, 53–54 (2004).
102. Tattersall, I. in: *Handbook of Paleoanthropology, 2nd ed.* (Henke, W. & Tattersall, I.) 2167–2187 (Springer, 2015).
103. Kaifu, Y. et al. New reconstruction and morphological description of a *Homo erectus* cranium: Skull IX (Tjg-1993.05) from Sangiran, Central Java. *J. Hum. Evol*. **61**, 270–294 (2011).

104. Wu, X., Schepartz, L. A., Falk, D. & Liu, W. Endocranial cast of Hexian *Homo erectus* from South China. *Am. J. Phys. Anthropol*. **130**, 445–454 (2006).

105. Cui, Y. & Wu, X. A geometric morphometric study of a Middle Pleistocene cranium from Hexian, China. J. *Hum. Evol.* **88**, 54–69 (2015).

106. Godinho, R. & O'Higgins P. in: *Human Remains: Another Dimension. The Application of Imaging to the Study of Human Remains* (Errickson, T. & Thompson, T.) 135–147 (2017).

107. Hublin, J.-J. et al. New fossils from Jebel Irhoud, Morocco and the pan-African origin of *Homo sapiens*. *Nature* **546**, 289–292 (2017).

108. Clarke, R.J. Latest information on Sterkfontein's *Australopithecus* skeleton and a new look at *Australopithecus*. *S. Afr. J. Sci.* **104**, 443–449 (2008).

109. Alemseged, Z. Reappraising the palaeobiology of *Australopithecus. Nature* **617**, 45–54 (2023).

110. Clarke, R.J. A *Homo habilis* maxilla and other newly-discovered hominid fossils from Olduvai Gorge, Tanzania. *J. Hum. Evol*. **63**, 418–428 (2012).

111. Zaim Y. et al. New 1.5 million-year-old *Homo erectus* maxilla from Sangiran (Central Java, Indonesia). *J. Hum. Evol*. **61**, 363–376 (2011).

112. Zollikofer, C.P.E., Beyrand, V., Lordkipanidze, D., Tafforeau, P. & Ponce de León, M. S. Dental evidence for extended growth in early *Homo* from Dmanisi. *Nature* **635**, 906–911 (2024).

113. Moggi-Cecchi, J., Grine, F.E. & Tobias, P.V. Early hominid dental remains from Members 4 and 5 of the Sterkfontein Formation (1966-1996 excavations): Catalogue, individual associations, morphological descriptions and initial metrical analysis. *J. Hum. Evol.* **50**, 239–328 (2006).

114. Tobias, P.V. *Olduvai Gorge. The Skulls Endocasts and Teeth of* Homo habilis (Cambridge University Press, 1991).

115. Moggi-Cecchi, J., Menter, C., Boccone, S. & Kayser, A. Early hominin dental remains from the Plio-Pleistocene site of Drimolen, South Africa. *J. Hum. Evol*. **58**, 374–405 (2010).

116. Leece, A.B. et al. New hominin dental remains from the Drimolen Main Quarry, South Africa (1999–2008). *Am. J. Biol. Anthropol*. 179, 240–260 (2022).

117. Martinón-Torres, M. et al. Dental remains from Dmanisi (Republic of Georgia): Morphological analysis and comparative study. *J. Hum. Evol*. **55**, 249–273 (2008).

118. Kaifu, Y. et al. Descriptions of the dental remains of *Homo floresiensis*. Anthropol. Sci. 123, 129–145 (2015).
119. Kaifu, Y., Aziz, F. & Baba, H. Hominid mandibular remains from Sangiran: 1952–1986 collection. *Am. J. Phys. Anthropol.* **128**, 497–519 (2005).
120. Ruff, C.B., Burgess, M.L., Ketcham, R.A. & Kappelman, J. Limb bone structural proportions and locomotor behavior in A.L. 288-1 ("Lucy"). *PLoS One* **11**, e0166095 (2016).
121. Lague, M.R. et al. Cross-sectional properties of the humeral diaphysis of *Paranthropus boisei*: Implications for upper limb function. *J. Hum. Evol*. **126**, 51–70 (2019).
122. Lague, M.R. Another massive distal humerus of *Paranthropus boisei* from Koobi Fora, Kenya. *Am. J. Phys. Anthropol*. **168** (S68), 134 (2019).
123. Cazenave, M. et al. Inner structural organization of the distal humerus in *Paranthropus* and *Homo*. *C. R. Palevol* **16**, 521–532 (2017).
124. Di Vicenzo, F. et al. The massive fossil humerus from the Oldowan horizon of Gombore I, Melka Kunture (Ethiopia, >1.39 Ma). *Quat. Sci. Rev*. **122**, 207–221 (2015).
125. Lague, M.R. & Menter, C.G. DNH 32: A distal humerus of *Paranthropus robustus* from Drimolen, South Africa. *Am. J. Phys. Anthropol.* **162** (S64), 255 (2017).
126. Kaifu, Y. et al. Early evolution of small body size in *Homo floresiensis*. *Nat. Commun*. **15**, 6381 (2024).